CH and PC bond activations of PMe$_2$Ph ligands by an octahedral Ru$_6$ cluster

Richard D. Adams *, Burjor Captain, Wei Fu, Mark D. Smith

Department of Chemistry and Biochemistry, University of South Carolina, 631 Sumter Street GRSC 109, 29208 Columbia, SC, USA

Abstract

The compound Ru$_6$(CO)$_{15}$(PMe$_2$Ph)$_2$(μ_6-C) (**1**) was obtained from the reaction of Ru$_6$(CO)$_{17}$(μ_6-C) with PMe$_2$Ph. Compound **1** exists in solution as a mixture of two slowly interconverting isomers. It is decarbonylated by treatment with Me$_3$NO·2H$_2$O to yield two new products Ru$_6$(CO)$_{13}$(μ-PMe$_2$)(μ_3-η^3-Me$_2$PC$_6$H$_4$)(μ_6-C) (**2**) and Ru$_6$(CO)$_{14}$(PMe$_2$Ph)(μ-η^2-MePhPCH$_2$)(μ_6-C)(μ-H) (**3**). Compound **2** is also obtained from **1** by thermal decarbonylation at 127 °C together with two additional compounds: Ru$_6$(CO)$_{14}$(μ-PMe$_2$)(μ-η^2-MePhPCH$_2$)(μ_6-C) (**4**) and Ru$_6$(CO)$_{12}$(μ-PMe$_2$)$_2$(μ_3-η^2-C$_6$H$_4$)(μ_6-C) (**5**). Compound **2** reacts reversibly with CO to form the CO adduct Ru$_6$(CO)$_{14}$(μ-PMe$_2$)(μ-η^2-Me$_2$PC$_6$H$_4$)(μ_6-C) (**6**). The structures of compounds **1**–**6** were established crystallographically. All contain octahedral Ru$_6$ clusters with a carbido ligand in the center. Except for **1**, all contain phosphine ligands in various stages of degradation. Compound **2** contains one bridging PMe$_2$ ligand formed by loss of a phenyl ring from a PMe$_2$Ph ligand and a bridging η^3-Me$_2$PC$_6$H$_4$ ligand formed by ortho-metallation of the phenyl ring of the second PMe$_2$Ph ligand. Compound **3** contains a bridging η^2-MePhPCH$_2$ ligand formed by metallation of one of the methyl groups of a PMe$_2$Ph ligand. Compound **4** contains a bridging PMe$_2$ and a bridging η^2-MePhPCH$_2$ ligand. Compound **5** contains two bridging PMe$_2$ ligands and a bridging (μ_3-η^2-C$_6$H$_4$) benzyne ligand fromed by cleavage of a phenyl ring from one of the PMe$_2$Ph ligands. Compound **6** contains one bridging PMe$_2$ ligand and a bridging η^2-Me$_2$PC$_6$H$_4$ ligand formed by ortho-metallation of the phenyl ring of one of the PMe$_2$Ph ligands. © 2002 Elsevier Science B.V. All rights reserved.

Keywords: Ruthenium; Cluster; Benzyne; Ortho-metallation; Cyclometallation; P–C cleavage

1. Introduction

It is well known that tertiary arylphosphine ligands can be converted thermally into phosphido bridges and orthometallated species by cleavage of P–C or C–H bonds on the ligand and formation of new M–P or M–C bonds. These types of transformations are recognized as some of the principal causes of deactivation in homogeneous transition metal catalysts that contain phosphine ligands [1]. The terms 'ortho-metallation' and 'cyclometallation' have been used to describe intramolecular metallations of phenyl rings at ortho-positions on ligands to form a chelate ring containing a metal–carbon bond [2]. Similar metallations of alkyl substituents of phosphine ligands have also been reported [1,3]. Pyrolysis of arylphosphine derivatives of Ru$_3$(CO)$_{12}$ and Os$_3$(CO)$_{12}$ has yielded a variety of novel complexes formed by degradation of the tertiary phosphine and by cluster expansion [4].

Metal carbonyl clusters containing an interstitial carbido ligand are of interest because the carbido ligand can stabilize the cluster toward reactions that might otherwise lead to its degradation [5]. The hexanuclear cluster Ru$_6$(CO)$_{17}$(μ_6-C) has been shown to react with phosphines to afford a variety of substituted derivatives [6,7]. In this report we describe the synthesis, structural analysis of the compound Ru$_6$(CO)$_{15}$(PMePh$_2$)$_2$(μ_6-C), and our studies of its thermal transformations into a variety of new complexes formed by intramolecular transformations of its phosphine ligands.

* Corresponding author. Tel.: +1-803-777-7187; fax: +1-803-777-6781.

E-mail address: adams@mail.chem.sc.edu (R.D. Adams).

2. Results and discussion

$Ru_6(CO)_{17}(\mu_6-C)$ reacts with two equivalents of PMe_2Ph at room temperature to yield the bis–phosphine derivative $Ru_6(CO)_{15}(PMe_2Ph)_2(\mu_6-C)$ (**1**) (72%). Brown et al. have made a number of other phosphine and phosphite derivatives of $Ru_6(CO)_{17}(\mu_6-C)$ by similar treatments [7]. Compound **1** was characterized by a combination of IR, NMR, mass spectrometry and single crystal X-ray diffraction analyses. An ORTEP diagram of the molecular structure of **1** is shown in Fig. 1. Compound **1** consists of an octahedral cluster of six ruthenium atoms with a carbido carbon atom in the center. The PMe_2Ph ligands are terminally coordinated to two adjacent Ru atoms. Interestingly, the ^{1}H- and ^{31}P-NMR spectrum of **1** at 25 °C indicates that it exists in solution as a mixture of two isomers hereafter referred to as **1a** and **1b** in a 4:1 ratio. Isomer **1a** shows a single doublet in the ^{1}H-NMR spectrum at 2.04 ppm, $^2J_{PH} = 10$ Hz which is assigned to the methyl groups and a singlet at 6.60 ppm in the $^{31}P\{^1H\}$ spectrum. Isomer **1b** shows a single doublet in the ^{1}H-NMR spectrum at 2.02 ppm for its methyl groups and a singlet 7.94 ppm in the $^{31}P\{^1H\}$ spectrum. The major isomer **1a** is assumed to be the structure found in the solid state. By symmetry all methyl groups of the isomer observed in the solid state are inequivalent. The observation of a single doublet for the methyl groups could, however, be achieved by an averaging process involving a localized scrambling of the three ligands on each of the phosphine substituted metal atoms. If there is indeed localized scrambling as indicated by the ^{1}H-NMR spectrum, then the only way to create a second distinguishable isomer would be to
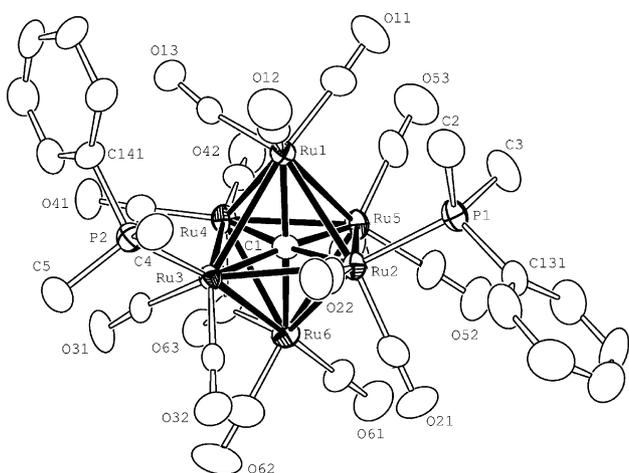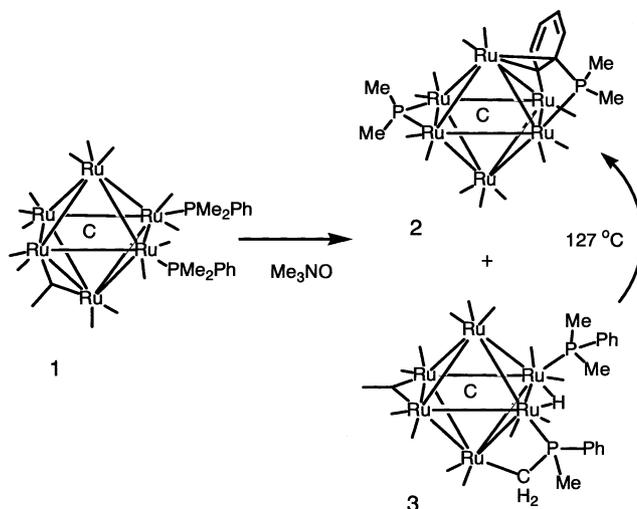
have the two phosphine ligands on oppositely positioned metal atoms (i.e. *trans* to one another). This is our proposed structure of **1b**. Curiously, the 2D EXSY ^{31}P-NMR spectrum for **1** shows cross peaks between the resonances of **1a** and **1b** at 90 °C indicating that they too are in a dynamic equilibrium at this temperature, but it is still relatively slow since there were no observable line broadening at this temperature. The mechanism of isomerization of **1a** and **1b** has not been established, but we have recently shown that the phosphine substituted octahedral cluster complex $PtRu_5(CO)_{15}(PMe_2Ph)(\mu_6-C)$ exists in solution as a mixture of two isomers that interconvert at elevated temperature by a mechanism that was shown unequivocally to occur by intramolecular phosphine migration [8]. Due to the strong similarity of **1** to $PtRu_5(CO)_{15}(PMe_2Ph)(\mu_6-C)$, we believe that an intramolecular phosphine shift mechanism could also be operative for the isomerization of **1a** and **1b**. Similar isomerism was proposed for other bis–phosphine derivatives of $Ru_6(CO)_{17}(\mu_6-C)$ [7].

1a   **1b**
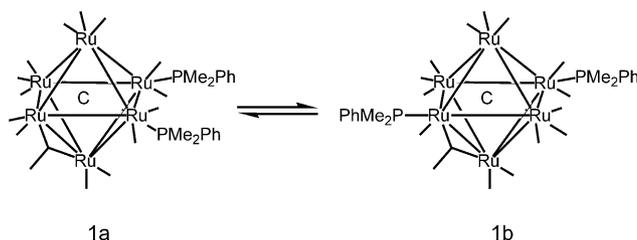
The reaction of **1** with $Me_3NO\cdot2H_2O$ at 25 °C afforded two new products $Ru_6(CO)_{13}(\mu-PMe_2)(\mu_3-\eta^3-Me_2PC_6H_4)(\mu_6-C)$ (**2**) and $Ru_6(CO)_{14}(PMe_2Ph)(\mu-\eta^2-MePhPCH_2)(\mu_6-C)(\mu-H)$ (**3**) in 11% and 37% yields, respectively, see Scheme 1. Both compounds were characterized by a combination of IR, NMR, and single crystal X-ray diffraction analyses. ORTEP diagrams for compounds **2** and **3** are shown in Figs. 2 and 3,

Fig. 1. An ORTEP diagram of $Ru_6(CO)_{15}(PMe_2Ph)_2(\mu_6-C)$ (**1**) showing 40% probability thermal ellipsoids. Selected bond distances (Å) and angles (°): Ru(1)–C(1) = 2.050(13) Ru(1)–Ru(5) = 2.9417(16), Ru(1)–Ru(3) = 2.9887(15), Ru(4)–C(1) = 2.093(12) Ru(1)–Ru(2) = 2.8386(15), Ru(2)–Ru(6) = 3.0938(15), Ru(2)–P(1) = 2.350(4), Ru(3)–P(2) = 2.368(4), O–C(av) = 1.151(16); P(1)–Ru(2)–Ru(1) = 99.84(11), P(1)–Ru(2)–Ru(6) = 147.62(11), Ru(1)–Ru(4)–Ru(5) = 61.77(4), C(1)–Ru(6)–Ru(2) = 41.0(3).

Scheme 1.
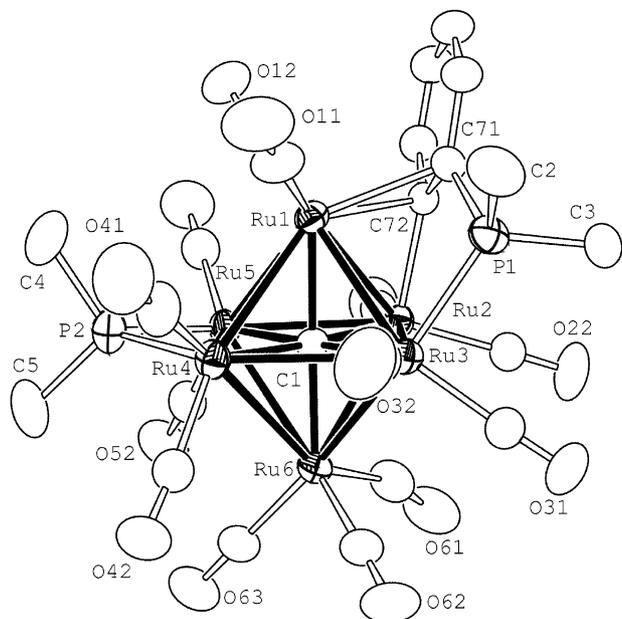
Fig. 2. An ORTEP diagram of $Ru_6(CO)_{13}(PMe_2)(Me_2PC_6H_4)(\mu_6\text{-}C)$ (**2**) showing 40% probability thermal ellipsoids. Selected bond distances (Å) and angles (°): Ru(1)–C(72) = 2.315(4), Ru(1)–C(71) = 2.342(4), Ru(2)–C(72) = 2.093(3), Ru(3)–P(1) = 2.2857(11), Ru(4)–P(2) = 2.2773(11), Ru(5)–P(2) = 2.2695(12), P(1)–C(71) = 1.813(4), P(1)–C(2) = 1.818(4), P(2)–C(4) = 1.810(5); P(1)–Ru(3)–Ru(1) = 70.86(3), P(1)–Ru(3)–Ru(4) = 125.31(3), P(2)–Ru(4)–Ru(5) = 51.27(3), P(2)–Ru(4)–Ru(1) = 92.12(3), P(2)–Ru(5)–Ru(2) = 140.98(3), P(2)–Ru(5)–Ru(4) = 51.51(3).
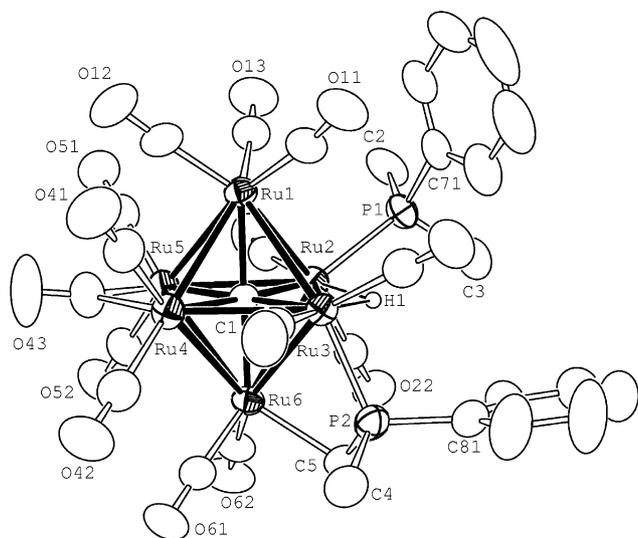

Fig. 3. An ORTEP diagram of $Ru_6(CO)_{14}(PMe_2Ph)(MePhPCH_2)(\mu_6\text{-}C)(\mu\text{-}H)$ (**3**) showing 40% probability thermal ellipsoids. Selected bond distances (Å) and angles (°): Ru2–Ru3 = 2.9498(5), Ru6–C5 = 2.184(5), Ru(2)–H(1) = 1.82(5), Ru(3)–H(1) = 1.84(5), Ru(6)–C(5) = , P(1)–C(71) = 1.811(6), P(2)–C(5) = 1.759(6), P(2)–C(4) = 1.814(5), P(2)–C(81) = 1.829(6), Ru(2)–P(1) = 2.3769(14), Ru(3)–P(2) = 2.3020(14), P(1)–C(3) = 1.824(5); C(5)–P(2)–C(4) = 105.7(3), O(32)–C(32)–Ru(4) = 120.2(4), O(43)–C(43)–Ru(5) = 140.4(4), O(43)–C(43)–Ru(4) = 133.4(4).

respectively. Compound **2** can be considered as a product of decarbonylation and ortho-metallation of a phenyl ring of one of the phosphine ligands. The second phosphine ligand has lost its phenyl ring completely and it has been eliminated from the complex, probably as benzene, formed by combination with the hydrogen atom that was cleaved from the metallated phenyl ring of the other phosphine ligand. Metallations and phenyl cleavages have been seen previously in the pyrolysis of other Ru and Os phosphine cluster complexes [4]. The phosphine ligand that lost its phenyl ring was transformed into a PMe_2 phosphido ligand that bridges the Ru(4) and Ru(5) metal–metal bond of the cluster, Ru(4)–P(2) = 2.2696(11) Å and Ru(5)–P(2) = 2.2696(12) Å, and serves as a $3e^-$ donor. The metallated phenyl ring is σ-bonded to the metal Ru(2), Ru(2)–C(72) = 2.093(3) Å, and η^2–π bonded to Ru(1), Ru(1)–C(72) = 2.315(4) Å, Ru(1)–C(71) = 2.342(4) Å. Together with the donation from the phosphorus atom, this ligand serves formally as a $5e^-$ donor. Similarly coordinated o-metallated phenyl groups were observed in the compounds $Ru_3\{\mu_3\text{-}PPh(\eta^1,\eta^2\text{-}C_6H_4)(\eta\text{-}C_5H_4)\text{-}Fe(\eta\text{-}C_5H_4PPh_2)(CO)_8(\mu\text{-}H)$ [9] and $Os_3(CO)_9[\mu_3\text{-}PPhMe(\eta^1,\eta^2\text{-}C_6H_4)](\mu\text{-}H)$ [10].

Compound **3** consists of a Ru_6 octahedron with one PMe_2Ph ligand terminally coordinated to ruthenium atom Ru(2). The other phosphine ligand has undergone a metallation of one of its methyl groups by cleavage of one of its C–H bonds. The hydrogen atom became a hydride ligand that bridges the two ruthenium atoms Ru(2) and Ru(3). The methylene group is metallated at ruthenium Ru(6), Ru(6)–C(5) = 2.184(5) Å. A chelate ring results in a shortening of the metal–phosphorus bond, Ru(3)–P(2) = 2.3019(14) Å, which is significantly shorter than the metal–phosphorus distance to the unchanged phosphine ligand P(1), Ru(2)–P(1) = 2.3769(14) Å. Interestingly, the phosphorus–carbon bond to the metallated carbon atom C(5) has become significantly shorter than the phosphorus–carbon bond to the unchanged methyl group C(4), P(2)–C(5) = 1.759(6) Å, P(2)–C(4) = 1.814(5) Å. The hydride ligand was located and refined crystallographically. It bridges the Ru(2)–Ru(3) bond. Ru(2)–H(1) = 1.82(5) Å, Ru(3)–H(1) = 1.84(5) Å. The Ru(2)–Ru(3) distance of 2.9496(5) Å, is slightly longer than the average Ru–Ru bond distance in the cluster. It is well established that bridging hydride ligands elongate metal–metal bonds. The ^{1}H-NMR spectrum shows resonances at −19.52 and −20.18 ppm confirming the presence of a hydride ligand, but also indicating that this compound also exists in solution as more than one isomer. This was further confirmed by variable temperature NMR studies, which showed broadening and averaging of the resonances, but a complete determination of the structures of the isomers and the mechanism(s) of their isomerization could not be established.
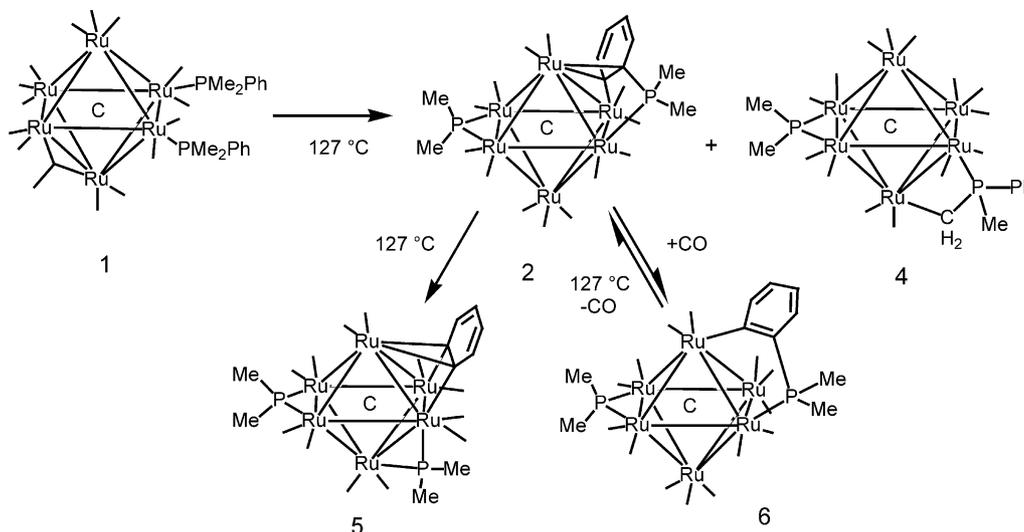
Scheme 2.

When refluxed in octane at 127 °C for 12 h, compound **1** was transformed into **2** in a better yield (61%) and two new compounds $Ru_6(CO)_{14}(\mu\text{-}PMe_2)(\mu\text{-}\eta^2\text{-}MePhPCH_2)(\mu_6\text{-}C)$ (**4**) (11%), and $Ru_6(CO)_{12}(PMe_2)_2(\mu_3\text{-}\eta^2\text{-}C_6H_4)(\mu_6\text{-}C)$ (**5**) (17%) were also formed in low yields, see Scheme 2. Compounds **4** and **5** were also characterized by a combination of IR, NMR, elemental and single crystal X-ray diffraction analyses. ORTEP diagrams of **4** and **5** are shown in Figs. 4 and 5, respectively. Compounds **4** and **5** both consist also of an octahedral cluster of six ruthenium atoms with a carbon atom in the center.

Compound **4** can be viewed as a benzene elimination product of **3**. It has the same methylene coordination as seen in **3**, however, now there is a bridging phosphido group formed by cleavage of the phenyl group which probably combined with the hydride to form benzene as in the formation of product **2**.

Compound **5** has two bridging phosphido groups, one bridging the Ru(4)–Ru(5) bond, and another bridging the Ru(3) and Ru(6) bond. In this case, both phosphine

Fig. 4. An ORTEP diagram of $Ru_6(CO)_{14}(PMe_2)(MePhPCH_2)(\mu_6\text{-}C)$ (**4**) showing 40% probability thermal ellipsoids. Selected bond distances (Å) and angles (°): Ru(3)–P(1) = 2.3148(18), Ru(4)–P(2) = 2.2774(15), Ru(5)–P(2) = 2.2611(16), Ru(6)–C(62) = 1.860(6), Ru(6)–C(61) = 1.860(7), P(1)–C(2) = 1.713(7), P(1)–C(3) = 1.795(7), P(1)–C(71) = 1.825(7), P(2)–C(4) = 1.799(7), P(2)–C(5) = 1.810(6); P(2)–Ru(5)–Ru(4) = 51.62(4), P(1)–Ru(3)–Ru(2) = 107.62(5), C(2)–P(1)–C(3) = 105.0(4), C(4)–P(2)–C(5) = 102.1(4), C(4)–P(2)–Ru(5) = 120.1(3), C(5)–P(2)–Ru(5) = 119.1(3), P(1)–C(2)–Ru(6) = 96.6(3), Ru(5)–P(2)–Ru(4) = 77.27(5).
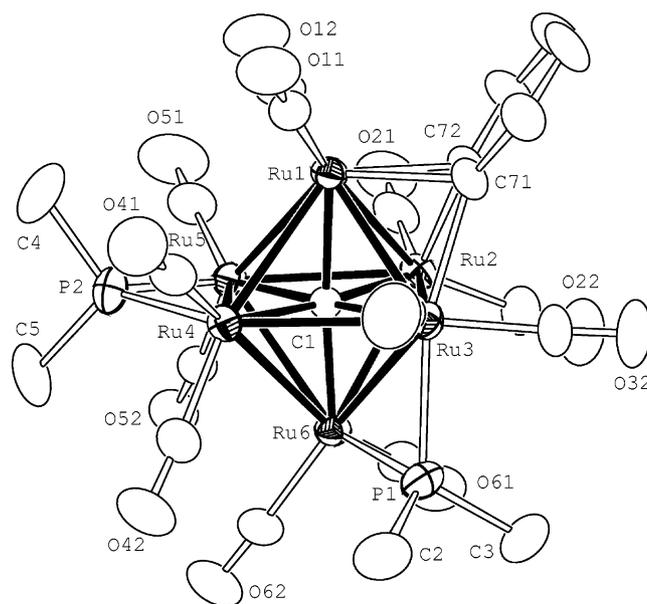
Fig. 5. An ORTEP diagram of $Ru_6(CO)_{12}(PMe_2)_2(\mu_3\text{-}\eta^2\text{-}C_6H_4)(\mu_6\text{-}C)$ (**5**) showing 40% probability thermal ellipsoids. Selected bond distances (Å) and angles (°): Ru(6)–P(1) = 2.2575(17), P(1)–C(2) = 1.810(7), P(1)–C(3) = 1.814(6), P(2)–C(5) = 1.809(7), P(2)–C(4) = 1.822(7) Ru(3)–C(71) = 2.217(6), Ru(2)–C(72) = 2.057(6), Ru(1)–C(71) = 2.156(6), Ru(1)–C(72) = 2.256(6); C(2)–P(1)–C(3) = 100.7(4), P(2)–Ru(4)–Ru(5) = 51.81(5), C(5)–P(2)–C(4) = 103.4(4) Ru(4)–P(2)–Ru(5) = 76.43(5), P(1)–Ru(3)–Ru(4) = 87.77(5) P(2)–Ru(5)–Ru(2) = 140.64(5).

ligands have undergone loss of their phenyl rings to form the phosphido groups. Most interestingly, one of the C_6 rings was not expelled, but was instead converted into a μ_3,η^2-triply bridging C_6H_4 benzyne ligand. These ligands have been observed to form by cleavage of phenyl rings from phosphine ligands for a variety of metal cluster complexes [11]. It bridges the Ru(1)–Ru(2)–Ru(3) triangular face of the octahedron and serves formally as a 4e$^-$ donor.

Compound **2** reacts with CO to form a stable CO adduct $Ru_6(CO)_{14}(\mu\text{-}PMe_2)(\mu\text{-}\eta^2\text{-}Me_2PC_6H_4)(\mu_6\text{-}C)$ (**6**) in 60% yield. An ORTEP diagram of the molecular structure of **6** is shown in Fig. 6. The structure of compound **6** is very similar to that of compound **2**, except the ortho-metallated phenyl ring is bonded to the cluster by only one carbon atom. Ru(2) has gained one CO ligand. The σ-bonded carbon atom of the phenyl ring is coordinated to Ru(2) and the metallated phosphine ligand was transformed from a 5e$^-$ donor in **2** to a 3e$^-$ donor in **6**. When compound **6** was heated to 127 °C, CO was eliminated and it was converted back to **2** in 77% yield. The transformations **6** to **2** to **5** provide a sequence of steps that shows a mechanism for cleavage of a phenyl ring from a phosphine ligand and its conversion into a bridging benzyne ligand in unprecedented detail.

Fig. 6. An ORTEP diagram of $Ru_6(CO)_{14}(PMe_2)(Me_2PC_6H_4)(\mu_6\text{-}C)$ (**6**) showing 40% probability thermal ellipsoids. Selected bond distances (Å) and angles (°): Ru(1)–C(72) = 2.127(3), Ru(5)–P(2) = 2.2677(10) P(1)–C(71) = 1.800(4), P(2)–C(4) = 1.811(4), P(2)–C(5) = 1.816(4), Ru(4)–P(2) = 2.2726(10), C(2)–P(1)–Ru(3) = 114.10(13), C(3)–P(1)–Ru(3) = 112.79(13), C(4)–P(2)–C(5) = 102.02(19), C(5)–P(2)–Ru(5) = 120.17(14), C(4)–P(2)–Ru(4) = 118.45(14), C(5)–P(2)–Ru(4) = 121.00(14), Ru(5)–P(2)–Ru(4) = 77.07(3).
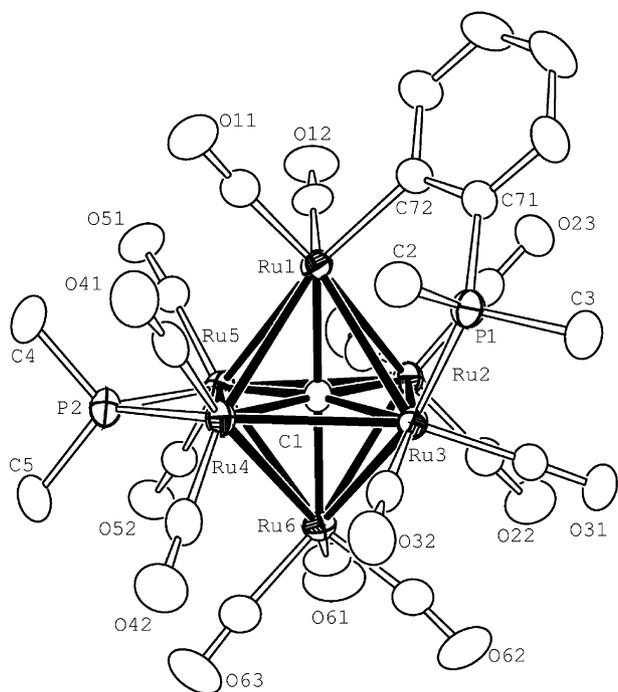
3. Experimental

3.1. General data

All reactions were performed under a nitrogen atmosphere. Reagent grade solvents were dried by the standard procedures and were freshly distilled prior to use. Infrared spectra were recorded on a Nicolet 5DXBO FTIR spectrophotometer. ^{1}H-NMR and ^{31}P-NMR were recorded on a Varian Inova 400 spectrometer operating at 400.1 and 161.9 MHz, respectively. ^{31}P-NMR spectra were externally referenced against 85% *ortho*-H_3PO_4. Variable temperature and 2D NOESY ^{31}P spectra were recorded on a Varian Inova 500 spectrometer operating at 202.49 MHz. Elemental analyses were performed by Desert Analytics (Tucson, AZ). $Ru_6(CO)_{17}(\mu_6\text{-}C)$ are prepared according to the published procedure [12]. PMe_2Ph and $Me_3NO\cdot2H_2O$ were purchased from Aldrich, and were used without further purification. The products were isolated by TLC in air on Analtech 0.25 and 0.50 mm silica gel 60 Å F_{254} glass plates.

3.2. Synthesis of $Ru_6(CO)_{15}(PMe_2Ph)_2(\mu_6\text{-}C)$ (1)

A mixture of 50.0 mg of $Ru_6(CO)_{17}(\mu_6\text{-}C)$ (0.045 mmol) and 13 μl of PMe_2Ph (0.091 mmol) was dissolved in 50 ml of CH_2Cl_2 in a 100 ml three-neck round-bottom flask. The solution was stirred at room temperature (r.t.) for 10 min, and the solvent was removed in vacuo. The products were separated by TLC by using a 3:1 hexane–methylene chloride solvent mixture to yield 43.0 mg (72%) of the red product, $Ru_6(CO)_{15}(PMe_2Ph)_2(\mu_6\text{-}C)$ (**1**). Spectral Data for **1** (a mixture of two isomers): IR ν_{CO} (cm^{-1} in CH_2Cl_2): 2064 (m), 2015 (vs), 1965 (w, sh), 1821 (w, br). ^{1}H-NMR (CDCl$_3$ in ppm): Ratio of Major Isomer **1a**:Minor Isomer **1b** = 4:1 at 25 °C. For **1a**: δ = 7.35–7.55 (m, 5H, Ph), 2.04 (d, 6H, Me, $^2J_{PH}$ = 10 Hz). ^{31}P{^{1}H}-NMR (CDCl$_3$ δ in ppm): 6.60; for **1b**: ^{1}H-NMR (CDCl$_3$ in ppm): δ = 7.35–7.55 (m, 5H, Ph), 2.02 (d, 6H, Me, $^2J_{PH}$ = 10 Hz); ^{31}P{^{1}H}-NMR (CDCl$_3$ in ppm): 7.94. MS: parent ion m/z = 1315.

3.3. Reaction of 1 with $Me_3NO\cdot2H_2O$

$Ru_6(CO)_{15}(PMe_2Ph)_2(\mu_6\text{-}C)$ (**1**) (14.6 mg, 0.011 mmol) and 2.0 mg of $Me_3NO\cdot2H_2O$ (0.016 mmol) were dissolved in 10 ml of CH_2Cl_2 in a 25 ml three-neck round-bottom flask. The reaction mixture was stirred at r.t. for 1 h after which the solvent was removed in vacuo. The products were separated by TLC using a 3:1 hexane–methylene chloride solvent mixture to yield 1.4 mg (11%) of a brown–red product, $Ru_6(CO)_{13}(\mu\text{-}PMe_2)(\mu_3\text{-}\eta^3\text{-}Me_2PC_6H_4)(\mu_6\text{-}C)$ (**2**) and 5.3 mg (37%) of an orange–red product, $Ru_6(CO)_{14}(PMe_2Ph)(\mu\text{-}\eta^2\text{-}MePhPCH_2)(\mu_6\text{-}C)(\mu\text{-}H)$ (**3**). Spectral Data for **2**: IR

v_{CO} (cm^{-1} in CH$_2$Cl$_2$): 2054 (m), 2011 (vs). ^{1}H-NMR (d_6-acetone in ppm): δ 8.14 (m, 1H, Ph), 8.03 (m, 1H, Ph), 7.35 (m, 1H, Ph), 6.77 (m, 1H, Ph), 2.47 (d, 3H, Me, $^2J_{PH}$ 11 Hz), 2.45 (d, 3H, Me, $^2J_{PH}$ 11 Hz), 2.17 (d, 3H, Me, $^2J_{PH}$ 11 Hz), 1.72 (d, 3H, Me, $^2J_{PH}$ 11 Hz). ^{1}H-NMR (CDCl$_3$ in ppm): δ 8.11 (m, 1H, Ph), 7.66 (m, 1H, Ph), 7.19 (m, 1H, Ph), 6.59 (m, 1H, Ph), 2.26 (3H, Me, $^2J_{PH}$ 11 Hz), 2.24 (3H, Me, $^2J_{PH}$ 11 Hz), 1.93 (d, 3H, Me, $^2J_{PH}$ 11 Hz), 1.59 (d, 3H, Me, $^2J_{PH}$ 11 Hz). ^{31}P{^{1}H}-NMR (CDCl$_3$ in ppm): δ 314.8, −12.56. Anal. Calc. C 24.41, H 1.36; Found: C 24.80, H 1.12%. Spectral Data for **3**: IR v_{CO} (cm^{-1} in CH$_2$Cl$_2$): 2061 (m), 2025 (vs). ^{1}H-NMR (CDCl$_3$ in ppm): δ 7.15–7.65 (m, Ph), 0.6–2.2 (m, CH$_3$), −19.52 (s, hydride), −20.18 (s, hydride). ^{31}P{^{1}H}-NMR (CDCl$_3$ in ppm): δ 2.35, −0.80, −3.67, −5.61, −9.50, −44.69, −48.49, −71.63. Anal. Calc. C 28.91, H 1.71; Found: C 29.02, H 1.86%.

3.4. Thermolysis of 1

Compound **1** (35.0 mg, 0.027 mmol) was dissolved in 25 ml of octane in a three-neck flask equipped with a reflux condenser, and then heated to reflux for 12 h. After cooling, the solvent was removed in vacuo, and the products were then separated by TLC by using a 3:1 hexane–methylene chloride solvent mixture to yield 3.7 mg (11%) of an orange–red product, Ru$_6$(CO)$_{14}$(μ-PMe$_2$)(μ-η^2-MePhPCH$_2$)(μ_6-C) (**4**), 5.1 mg (17%) of a brown–red product, Ru$_6$(CO)$_{12}$(μ-PMe$_2$)$_2$(μ_3-η^2-C$_6$H$_4$)(μ_6-C) (**5**), and 19.1 mg (61%) of **2**. Spectral Data for **4**: IR v_{CO} (cm^{-1} in CH$_2$Cl$_2$): 2066 (m), 2022 (vs). ^{1}H-NMR (CD$_2$Cl$_2$ in ppm): δ 7.4–7.6 (m, Ph), 2.26 (d, 3H, Me, $^2J_{PH}$ 11 Hz), 2.23 (d, 3H, Me, $^2J_{PH}$ 11 Hz), 1.88 (d, 3H, Me, $^2J_{PH}$ 11 Hz), 0.85 (dd, 1H, CH$_2$, $^2J_{HH}$ 11 Hz, $^2J_{HH}$ 7 Hz), 0.48 (d, 1H, CH$_2$, $^2J_{HH}$ 11 Hz, $^2J_{HH}$ ∼ 0 Hz). ^{31}P{^{1}H}-NMR (CD$_2$Cl$_2$ in ppm): δ 328.15, −48.8. Anal. Calc. C 24.25, H 1.29; Found: C 24.42, H 1.53%. Spectral Data for **5**: IR v_{CO} (cm^{-1} in CH$_2$Cl$_2$): 2066 (m), 2012 (vs). ^{1}H-NMR (CDCl$_3$ in ppm): δ 8.61 (d, 1H, Ph), 8.34 (d, 1H, Ph), 6.83 (m, 2H, Ph), 2.33 (d, 3H, Me, $^2J_{PH}$ 11 Hz), 2.20 (d, 3H, Me, $^2J_{PH}$ 11 Hz), 2.07 (d, 3H, Me, $^2J_{PH}$ 11 Hz), 1.86 (d, 3H, Me, $^2J_{PH}$ 11 Hz). ^{31}P{^{1}H}-NMR (CDCl$_3$ in ppm): δ 311.32, 301.25. Anal. Calc. C 23.94, H 1.38; Found: C 24.56, H 1.23%.

3.5. Synthesis of Ru$_6$(CO)$_{14}$(μ-PMe$_2$)(μ-η^2-Me$_2$PC$_6$H$_4$)(μ_6-C) (6)

Compound **2** (12.3 mg, 0.010 mmol) was dissolved in 15 ml CH$_2$Cl$_2$. CO was then bubbled through the solution for 3 h. The solvent was then removed in vacuo, and the product was purified by TLC using a 3:1 hexane–methylene chloride solvent mixture to yield 6.0 mg (60%) of an orange–red product, Ru$_6$(CO)$_{14}$(μ-PMe$_2$)(μ-η^2-Me$_2$PC$_6$H$_4$)(μ_6-C) (**6**). Spectral data for **6**:

IR v_{CO} (cm^{-1} in CH$_2$Cl$_2$): 2066 (m), 2023 (s), 2015 (s, sh), 1969 (w). ^{1}H-NMR (d_6-acetone in ppm): δ 7.97 (m, 1H, Ph), 7.25 (m, 1H, Ph), 7.09 (m, 1H, Ph), 6.99 (m, 1H, Ph), 2.53 (d, 3H, Me, $^2J_{PH}$ 11 Hz), 2.48 (d, 3H, Me, $^2J_{PH}$ 11 Hz), 2.27 (d, 3H, Me, $^2J_{PH}$ 11 Hz), 1.96 (d, 3H, Me, $^2J_{PH}$ 11 Hz). ^{1}H-NMR (CDCl$_3$ in ppm): δ 7.96 (m, 1H, Ph), 20 (m, 1H, Ph), 6.93 (m, 1H, Ph), 6.80 (m, 1H, Ph), 2.26 (3H, Me, $^2J_{PH}$ 11 Hz), 2.24 (3H, Me, $^2J_{PH}$ 11 Hz), 2.10 (d, 3H, Me, $^2J_{PH}$ 11 Hz), 1.86 (d, 3H, Me, $^2J_{PH}$ 11 Hz). ^{31}P{^{1}H}-NMR (CDCl$_3$ in ppm): δ 324.18, −16.93. Anal. Calc. C 24.82, H 1.32. Found: C 25.18, H 1.20%.

3.6. Thermolysis of 6

Compound **6** (11.2 mg, 0.009 mmol) was dissolved in 15 ml of octane and brought to reflux for 30 min. After cooling, the solvent was removed in vacuo, and the products were separated by TLC by using a 3:1 hexane–methylene chloride solvent mixture to yield 9.0 mg (77%) of **2**, and trace amounts of **4** and **5**.

3.7. Crystallographic analyses

Red single crystals of compounds **1**–**6** suitable for diffraction analysis were grown by slow evaporation of solvent from a hexane–methylene chloride solution at 5 °C. The crystals selected for data collection were glued onto the ends of thin glass fibers. X-ray intensity data were measured at 293 K (**1**–**3**, **5**), 183 K (**4**) or 173 K (**6**) using a Bruker SMART APEX CCD-based diffractometer using Mo–K$_\alpha$ radiation ($\lambda = 0.71073$ Å) [13]. The raw data frames were integrated with the SAINT+ program, which also applied corrections for Lorentz and polarization effects. Empirical absorption corrections based on the multiple measurement of equivalent reflections were applied using the program SADABS. Crystal data, data collection parameters, and the results of the analyses are listed in Tables 1 and 2. All structures were solved by a combination of direct methods and difference Fourier syntheses, and refined by full-matrix least-squares on F^2, using the SHELXTL software package [14].

Compounds **1**, **2**, **4** and **5** crystallized in the monoclinic crystal system. The space groups $P2_1/c$ for **1**, **2** and **4** and $P2_1/n$ for **5** were identified uniquely on the basis of the systematic absences in the intensity data and were further confirmed by the successful solution and refinement of the structures. Compound **1** contains two independent formula equivalents of the complex in the asymmetric unit. Compound **3** crystallized in the triclinic crystal system. The space group $P\bar{1}$ was assumed and confirmed by the successful solution and refinement of the structure. Compound **3** contains a hydride ligand, which was located and refined with an isotropic thermal parameter. Compound **6** also crystal-

Table 1
Crystal data for compounds **1**–**3**

Compound	1	2	3
Empirical formula	$Ru_6P_2O_{15}C_{32}H_{22}$	$Ru_6P_2O_{13}C_{24}H_{16}$	$Ru_6P_2O_{14}C_{31}H_{22}$
Formula weight	1314.86	1180.73	1286.85
Crystal system	Monoclinic	Monoclinic	Triclinic
Lattice parameters			
a (Å)	10.6738(8)	11.979(1)	9.0107(4)
b (Å)	21.645(2)	1 293(1)	11.9545(6)
c (Å)	34.818(3)	16.274(1)	19.4022(9)
α (°)	90	90	92.478(1)
β (°)	93.914(2)	90.565(2)	98.313(1)
γ (°)	90	90	111.048(1)
V (Å³)	8025.5(10)	3371.0(4)	1919.8(2)
Space group	$P2_1/c$ (#14)	$P2_1/c$ (#14)	$P\bar{1}$ (#2)
Z value	8	4	2
ρ_{calc} (g m^{-3})	2.176	2.326	2.226
μ (Mo–K$_\alpha$) (mm^{-1})	2.345	2.773	2.447
Temperature (°C)	20	20	20
$2\Theta_{max}$ (°)	50.18	52.76	52.82
Number of observations ($I > 2\sigma(I)$)	8154	5427	5675
Number of parameters	999	410	493
Goodness-of-fit	1.029	0.913	0.896
Max. shift in cycle	0.003	0.001	0.001
Residuals: R; wR_2	0.0696; 0.1272	0.0276; 0.0606	0.0316; 0.0648
Absorption correction	SADABS	SADABS	SADABS
Transmissions coeffecient, Max/Min	0.962/0.806	0.656/0.504	0.837/0.533
Largest peak in final difference map (e Å^{-3})	1.097	1.007	0.807

Table 2
Crystal data for compounds **4**–**6**

Compound	4	5	6
Empirical formula	$Ru_6P_2O_{14}C_{25}H_{16}\cdot0.25CH_2Cl_2$	$Ru_6P_2O_{12}C_{23}H_{16}$	$Ru_6P_2O_{14}C_{25}H_{16}$
Formula weight	1229.97	1152.62	1208.74
Crystal system	Monoclinic	Monoclinic	Monoclinic
Lattice parameters			
a (Å)	16.9452(11)	10.3078(5)	39.160(3)
b (Å)	10.4252(6)	15.2357(8)	10.2589(7)
c (Å)	21.5604(13)	21.012(1)	18.787(1)
α (°)	90	90	90
β (°)	112.434(1)	102.402(1)	116.326(1)
γ (°)	90	90	90
V (Å³)	3520.5(4)	3222.9(3)	6764.7(8)
Space group	$P2_1/c$ (#14)	$P2_1/n$ (#14)	$C2/c$ (#15)
Z value	4	4	8
ρ_{calc} (g cm^{-3})	2.321	2.376	2.374
μ (Mo–K$_\alpha$) (mm^{-1})	2.699	2.895	2.769
Temperature (°C)	−90	20	−100
$2\Theta_{max}$ (°)	54.26	52.74	52.82
Number of observations ($I > 2\sigma(I)$)	6093	4839	5965
Number of parameters	450	392	428
Goodness-of-fit	1.006	0.936	0.975
Max. shift in cycle	0.001	0.001	0.001
Residuals: R; wR_2	0.0387; 0.1005	0.0387; 0.0722	0.0213; 0.0474
Absorption correction	SADABS	SADABS	SADABS
Transmissions coeffecient, Max/Min	0.92/0.69	0.914 / 0.798	0.902 / 0.735
Largest peak in Final difference map (e Å^{-3})	2.955	0.810	0.643

lized in the monoclinic crystal system. Systematic absences were consistent with the space groups $C2/c$ or Cc; intensity statistics indicated $C2/c$, which was confirmed by the successful solution and refinement of the structure. For each compound, all nonhydrogen atoms were refined with anisotropic thermal parameters; hydrogen atoms except for the hydride in **3** were placed in calculated positions and treated as standard riding atoms [14].

4. Supplementary material

Crystallographic data for the structural analysis has been deposited with the Cambridge Crystallographic Data Centre, CCDC 178189–178194 for compounds **1**–**6**, respectively. Copies of this information may be obtained free of charge from The Director, CCDC, 12 Union Road, Cambridge, CB2 1EZ, UK (Fax: +44-1223-336033, or e-mail: deposit@ccdc.cam.ac.uk or www: http://www.ccdc.cam.ac.uk.

Acknowledgements

References

[1] (a) P.E. Garrou, Chem. Rev. 85 (1985) 171;
(b) R.A. Dubois, P.E. Garrou, Organometallics 5 (1986) 460;
(c) G. Lavigne, in: D.F. Shriver, H.D. Kaesz, R.D. Adams (Eds.), Chemistry of Metal Cluster Complexes, VCH, Weinheim, 1990, p. 201.

[2] A. Ryabov, Chem. Rev. 90 (1990) 403.

[3] (a) D. Rabinovitch, R. Zelman, G. Parkin, J. Am. Chem. Soc. 114 (1992) 4611;
(b) A.J. Deeming, M. Underhill, J. Chem. Soc. Dalton Trans. (1973) 2727;

(c) A.J. Deeming, M. Underhill, J. Organomet.Chem. 128 (1977) 63.

[4] (a) M.I. Bruce, N.N. Zaitseva, B.W. Skelton, A.H. White, J. Organomet.Chem. 515 (1996) 143;
(b) C.W. Bradford, R.S. Nyholm, G.J. Gainsford, J.M. Guss, P.R. Ireland, R. Mason, J. Chem. Soc., Chem. Commun. (1972) 87;
(c) G.J. Gainsford, J.M. Guss, P.R. Ireland, R. Mason, C.W. Bradford, R.S. Nyholm, J. Organomet. Chem. 40 (1972) C70;
(d) A.J. Deeming, S.E. Kabir, M. Underhill, J. Chem. Soc. Dalton Trans. (1973) 2589;
(e) A.J. Deeming, I.P Rothwell, M.B. Hursthouse, J.D. Backer-Dirks, J. Chem. Soc. Dalton Trans. (1981) 1879;
(f) S.C. Brown, J. Evans, M.J. Webster, J. Chem. Soc. Dalton Trans. (1980) 1021;
(g) M.I. Bruce, G. Shaw, F.G.A. Stone, J. Chem. Soc. Dalton Trans. (1972) 2094.

[5] M. Tachikawa, E.L. Muetterties, Prog. Inorg. Chem. 28 (1981) 203.

[6] P. Dyson, Adv. Organomet. Chem. 43 (1999) 43.

[7] (a) S.C.Brown, J. Evans, M.J. Webster, J. Chem. Soc. Dalton Trans. (1981) 2263;
(b) B.F.G. Johnson, J. Lewis, J.N. Nicholls, J. Puga, P.R. Raithby, M. McPartlin, W. Clegg, J. Chem. Soc. Dalton Trans. (1983) 277.

[8] R.D. Adams, B. Captain, W. Fu, P.J. Pellechia, Chem. Commun. (2000) 937.

[9] W.R. Cullen, S.J. Retting, T.C. Zheng, Can. J. Chem. 70 (1992) 2215.

[10] A.J. Deeming, S.E. Kabir, N.I. Powell, P.A. Bates, M.B. Hursthouse, J. Chem. Soc. Dalton Trans. (1987) 1529.

[11] (a) S. Brait, S. Deabate, S.A.R. Knox, E. Sappa, J. Cluster Sci. 12 (2001) 139;
(b) S.A.R. Knox, B.R. Lloyd, D.A.V. Morton, S.M. Nicholls, A.G. Orpen, J.M. Vinas, M. Weber, G.K. Williams, J. Organomet. Chem. 394 (1990) 385;
(c) W.R. Cullen, S.T. Chacon, M.I. Bruce, F.W.B. Einstein, R.H. Jones, Organometallics 7 (1988) 2273;
(d) M.I. Bruce, P.A. Humprey, O.B. Shawkataly, M.R. Anow, E.R.T. Tiekink, W.R. Cullen, Organometallics 9 (1990) 2910.

[12] J.N. Nicholls, M.D. Vargas, J. hriljac, M. Sailor, Inorg. Synth. 26 (1989) 283.

[13] SMART Version 5.624, SAINT+ Version 6.02a and SADABS. Bruker Analytical X-ray System, Inc., Madison, Wisconsin, USA, 1998.

[14] G.M. Sheldrick, SHELXTL Version 5.1; Bruker Analytical X-ray Systems, Inc., Madison, Wisconsin, USA, 199.